SCIENCE CHINA
Physics, Mechanics & Astronomy

• Research Paper •

May 2010 Vol.53 No.5: 852–855
doi: 10.1007/s11433-010-0187-x

Oxygen vacancy induced magnetism in $BaTiO_{3-\delta}$ and Nb:$BaTiO_{3-\delta}$ thin films

YANG Fang, JIN KuiJuan, LU HuiBin*, HE Meng, WANG Cong, WEN Juan & YANG GuoZhen

Beijing National Laboratory for Condensed Matter Physics, Institute of Physics, Chinese Academy of Sciences, Beijing 100190, China

Received October 23, 2009; accepted December 21, 2009

The unusual magnetic properties are observed in oxygen deficient $BaTiO_{3-\delta}$ (BTO) and Nb:$BaTiO_{3-\delta}$ (BNTO) thin films fabricated on $SrTiO_3$ substrates by laser molecular beam epitaxy. The distinct magnetic hysteresis loops are observed in the oxygen deficient BTO and BNTO thin films in a temperature range of 5 to 300 K, whereas the diamagnetism is observed in both BTO and BNTO annealed at 1 atm of oxygen. The dopant Nb only enhances the magnetization in BNTO thin films, but has little effect on the coercivity. The magnetism of BTO and BNTO films is proposed to be the oxygen vacancies by origin.

oxygen vacancy, magnetism, $BaTiO_{3-\delta}$ (BTO), Nb:$BaTiO_{3-\delta}$ (BNTO), thin films

PACS: 75.70.-i, 75.47.Pq, 77.55.fe

1 Introdution

Perovskite oxides have been known to exhibit a broad range of technologically important properties, such as superconductivity [1,2], dielectric [3,4], colossal magnetoresistance [5–8], ferroelectric [9–11], and nonlinear optical properties [12], and thus become one of the key materials for multifunctional devices [13]. The physical properties of the perovskite oxides have been very much extended by the introduction of various defects [5,14,15]. Among them, the self-doping by oxygen vacancies is essential because the oxygen vacancy is one of the elemental and intrinsic defects in perovskite oxides and can greatly influence the oxide properties. For instance, oxygen vacancies can cause the insulator-to-metal transition in the perovskite oxide [16], and transform optical properties into visible-light emitting [17]. Sundaresan et al. [18] observed the ferromagnetism in nano-particles of nonmagnetic oxides such as CeO_2, Al_2O_3, ZnO, In_2O_3, and SnO_2. Shein et al. [19] predicted vacancy-induced magnetism in non-magnetic perovskite $SrTiO_{3-\delta}$. Besides, oxygen vacancies can be readily obtained in perovskite oxides either in the process of growing or through other processes such as annealing and redox reactions [20].

Barium Titanate ($BaTiO_3$), as a member of perovskite family, is one of the most extensively investigated oxide materials because of its abundant physical properties and potential applications. For years, doped $BaTiO_3$ materials have attracted great attention for their semi-conductive and conductive properties, and they are expected to have many device applications [21,22]. Previously we reported the epitaxy growth [23–25], structures [26], and physical properties [27,28] of doped $BaTiO_3$ and the oxygen deficient doped $BaTiO_3$ thin films. To our knowledge, so far no magnetic property has ever been directly detected in such non-magnetic perovskite oxide materials. This paper presents the very unusual and interesting property of magnetism induced by oxygen vacancies in the oxygen deficient $BaTiO_{3-\delta}$ (BTO) and Nb:$BaTiO_{3-\delta}$ (BNTO) thin films fabricated on $SrTiO_3$ (STO) substrates.

*Corresponding author (email: hblu@aphy.iphy.ac.cn)

2 Experiment

The oxygen deficient BTO and BNTO thin films are grown on STO (001) substrates by a laser molecular beam epitaxy. As mentioned in our previous reports [23–25], a focused pulsed XeCl excimer laser beam (~ 20 ns, 2 Hz, ~ 1.5 J/cm^2) is irradiated onto a sintered $BaTiO_3$ or a $BaNb_{0.3}Ti_{0.7}O_3$ target, respectively. The thin films are deposited at 620℃ under an oxygen pressure of 1×10^{-4} Pa. An *in situ* reflection high-energy electron diffraction (RHEED) and charge-coupled device (CCD) camera are used to monitor the growth process of the thin films. The intensity oscillation of RHEED not only enables us to precisely control the number of BTO or BNTO molecular layers during growth, but also shows that the films are layer-by-layer epitaxial growth. The thickness of the BTO and BNTO films are 300 nm determined from the RHEED oscillations. After deposition, the samples are *in situ* annealed at the deposition conditions for one hour.

3 Results and discussion

Figure 1 displays the X-ray diffraction (XRD) θ-2θ scan curves of BTO and BNTO thin films. Except for the diffraction peaks of BTO (00*l*) (or BNTO (00*l*)) and STO (00*l*), there are no diffraction peaks from impurity phase or randomly oriented grains, which implies that the BTO and BNTO thin films are single phase and *c* axis orientation.

The temperature dependence of resistance (*R*-*T*) for the as-prepared BTO and BNTO thin films is measured by a constant pulse-modulated current source in a temperature range of 10 K to 300 K. As shown in Figure 2, the BTO and BNTO thin films show metallic behavior. Hall measurements of the BTO and BNTO films are taken at room temperature. The resistivity, carrier concentration and the Hall coefficient are 2.84×10^{-4} Ω·cm, 4.53×10^{21} cm^{-3}, -1.56×10^{-3} cm^3/C for BTO film and 7.3×10^{-5} Ω·cm, 1.4×10^{22} cm^{-3}, -4.8×10^{-4} cm^3/C for BNTO film, respectively.

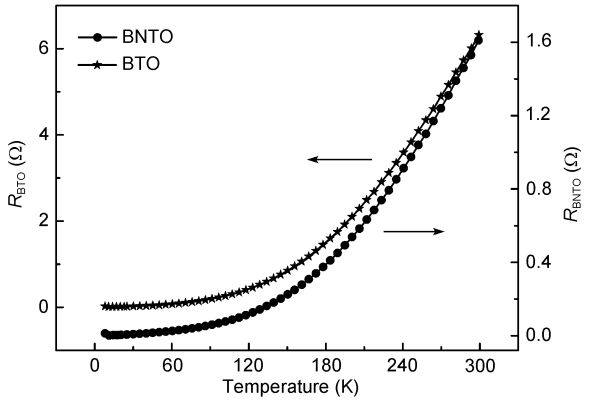

Figure 2 Temperature dependence of the resistance of the oxygen deficient BTO and BNTO thin films.

The novel property of the BTO films is the magnetic hysteresis loops observed in a temperature range of 5 K to 300 K. The magnetic hysteresis loops are measured by a superconducting quantum interference device (SQUID, Quantum Design MPMS-7). Figure 3 shows the magnetic hysteresis loops of the oxygen deficient BTO films at 5 K, 90 K and 300 K after the diamagnetic contribution from the STO substrate is eliminated. The applied magnetic field is parallel to the surface of the film. It can be seen that both the saturation magnetization (M_s) and coercivity (H_c) decrease with increasing temperature. The M_s and H_c are approximately 4.8×10^{-5} emu, 420 Oe at 5 K, 4.5×10^{-5} emu, 230 Oe at 90 K, and 3.8×10^{-5} emu, 150 Oe at 300 K, respectively. The temperature dependence of the hysteresis loop is consistent with the conventional magnetic behavior. The result indicates that the ferromagnetic order dominates

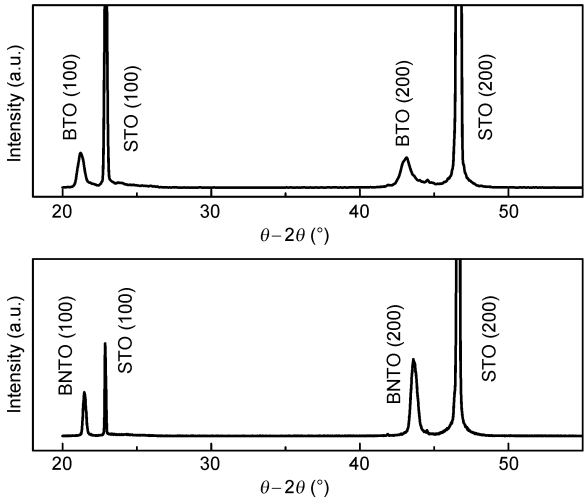

Figure 1 XRD θ-2θ scan curves of 300 nm oxygen deficient BTO and BNTO thin films on STO substrates.

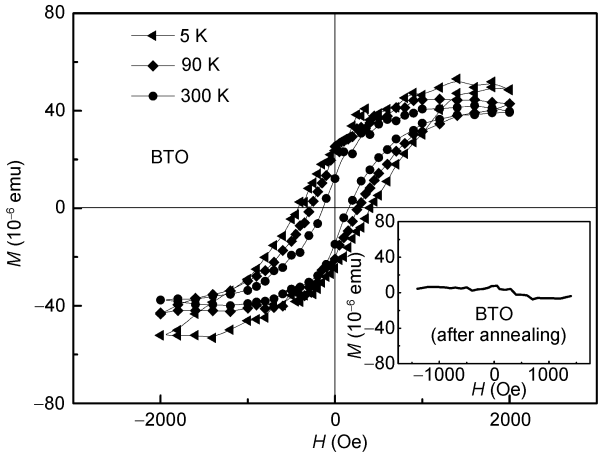

Figure 3 Magnetic hysteresis loops of the oxygen deficient BTO films at 5 K, 90 K, and 300 K. The inset shows the *M*-*H* curve of the annealed BTO film at 90 K.

the entire temperature range.

We suppose the origin of the magnetism in BTO is the oxygen vacancies. Thus, the BTO thin films are annealed in 1 atm of oxygen at 600℃ for 4 hours to reduce the oxygen vacancies in BTO films. The inset in Figure 3 shows the magnetization versus field (*M-H*) curve of the annealed BTO films at 90 K. The magnetic hysteresis loop disappears and shows a typical diamagnetic curve after annealing. The experimental results confirm that the magnetism in BTO may have been caused by the oxygen vacancies.

One possible origin of the magnetism is the interface effect. To eliminate this possibility, we have further measured the magnetic hysteresis loops of the BNTO/STO sample. The magnetization loops shown in Figure 4 is the magnetic response of the BNTO thin films after the contribution is eliminated from the STO substrate. The upper inset of Figure 4 displays the hysteresis loops of the whole sample of BNTO/STO and the diamagnetic response of the STO substrate at 90 K and 300 K. From the hysteresis in Figure 4, we can see that M_s and H_c are about 7.3×10^{-5} emu, 200 Oe at 90 K, and about 6.7×10^{-5} emu, 120 Oe at 300 K, respectively. The magnetization loops are evident in the temperature range of 90 K to 300 K. Since thin films with different interfaces show similar magnetic behavior, the interface effect can be eliminated. Similar to BTO, the BNTO films are also diamagnetic after annealing in oxygen ambience as shown in the lower inset of Figure 4. Furthermore, the magnetization of BNTO films is a little larger than that of BTO films, which implies that the dopant Nb can enhance the magnetization to some extent. However, the coercivity of BNTO films does not change very much, indicating that the magnetism of BNTO films equally originates from the oxygen vacancy.

Figure 5 displays the magnetization-temperature (*M-T*) curves of the BTO and BNTO samples under 5000 Oe magnetic field after eliminating the influence of the STO substrates. The oxygen deficient BTO and BNTO films show larger magnetization, and the dopant Nb can enhance the magnetism. On the other hand, the magnetism of both BTO and BNTO films decrease after annealing in oxygen and the curves are very close. The *M-T* results completely agree with the above hysteresis measurements.

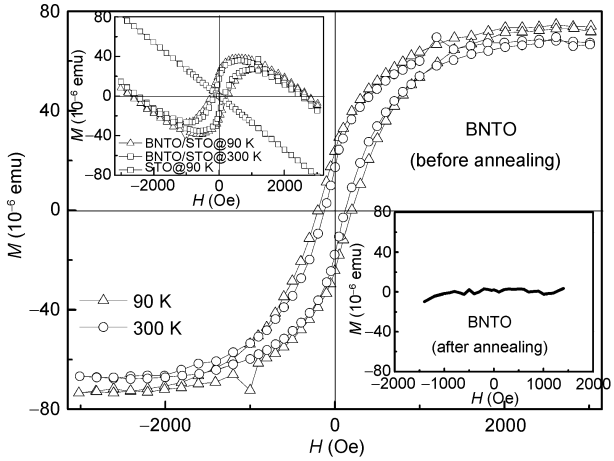

Figure 4 Magnetic hysteresis loops of the oxygen deficient BNTO thin films at 90 K and 300 K. The upper inset shows the hysteresis loop of the BNTO/STO sample and the diamagnetic response of the STO substrate. The lower inset shows the *M-H* curve of the annealed BNTO film at 90 K.

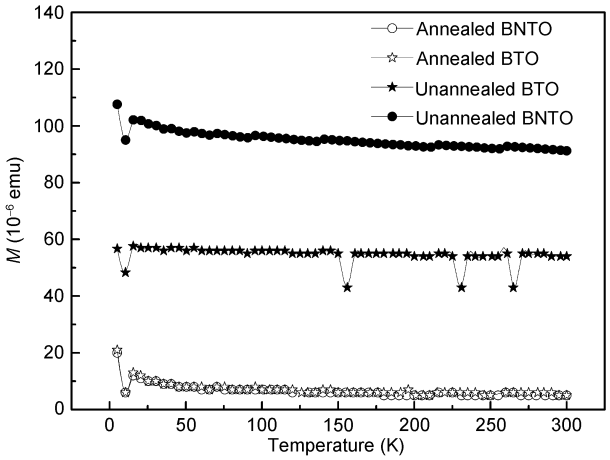

Figure 5 Magnetization-temperature curves of the BTO and BNTO samples under 5000 Oe magnetic field after eliminating the STO substrate influence.

The oxygen vacancies mentioned cause the magnetism in the oxygen deficient BTO and BNTO thin films. The experimental results are consistent with the prediction in ref. [19]. The oxygen vacancies not only cause metallic behavior for non-magnetic perovskite oxides but also introduce spin polarization of Ti atoms closest to the oxygen vacancy sites in BTO and BNTO thin films, so the magnetic effects in non-magnetic perovskite oxide material are observed.

4 Conclusions

In summary, we experimentally proved the unusual magnetic properties in the oxygen deficient BTO and BNTO thin films whereas the BTO and BNTO with enough oxygen exhibit diamagnetism. The magnetic hysteresis loops are clearly observed in the temperature range of 5 K to 300 K. Further studies on ferromagnetism property in other oxygen deficient perovskite oxides, such as $SrTiO_3$, $LaAlO_3$ and the like are highly expected. The present experimental results are expected to open up new possibilities in the investigations of the mechanism and the application for the perovskite oxides as well as spin electronics.

This work was supported by the National Natural Science Foundation of China (Grant No. 50672120) and the National Basic Research Program of China (Grant No. 2007CB307005).

1 Maeno Y, Hashimoto H, Yoshida K, et al. Superconductivity in a

layered perovskite without copper. Nature, 1994, 372: 532–534
2 Ohtomo A, Hwang H Y. A high-mobility electron gas at the $LaAlO_3$/$SrTiO_3$ heterointerface. Nature, 2004, 427: 423–426
3 Basceri C, Streiffer S K, Kingon A I, et al. The dielectric response as a function of temperature and film thickness of fiber-textured (Ba,Sr)TiO_3 thin films grown by chemical vapor deposition. J Appl Phys, 1997, 82: 2497–2504
4 Chang W, Horwitz J S, Carter A C, et al. The effect of annealing on the microwave properties of $Ba_{0.5}Sr_{0.5}TiO_3$ thin films. Appl Phys Lett, 1999, 74: 1033-1036
5 Lu H B, Yang G Z, Chen Z H, et al. Positive colossal magnetoresistance in a multilayer p-n heterostructure of Sr-doped LaMnO3 and Nb-doped $SrTiO_3$. Appl Phys Lett, 2004, 84: 5007–5010
6 Jin K J, Lu H B, Zhou Q L, et al. Positive colossal magnetoresistance from interface effect in p-n junction of $La_{0.9}Sr_{0.1}MnO_3$ and $SrNb_{0.01}Ti_{0.99}O_3$. Phys Rev B, 2005, 71: 184428
7 Lu H B, Dai S Y, Chen Z H, et al. High sensitivity of positive magnetoresistance in low magnetic field in perovskite oxide p-n junctions. Appl Phys Lett, 2005, 86: 032502
8 Mitra C, Raychaudhuri P, Dorr K, et al. Observation of minority spin character of the new electron doped manganite $La_{0.7}Ce_{0.3}MnO_3$ from tunneling magnetoresistance. Phys Rev Lett, 2003, 90: 017202
9 Wang J, Neaton J B, Zheng H, et al. Epitaxial $BiFeO_3$ multiferroic thin film heterostructures. Science, 2003, 299: 1719–1722
10 Cohen R E. Origin of ferroelectricity in perovskite oxides. Nature, 1992, 358: 136–138
11 Ahn C H, Rabe K M, Triscone J M. Ferroelectricity at the nanoscale: Local polarization in oxide thin films and heterostructures. Science, 2004, 303: 488–491
12 Sharan A, Lettieri J, Jia Y F, et al. Bismuth manganite: A multiferroic with a large nonlinear optical response. Phys Rev B, 2004, 69: 214109
13 Ahn C H, Bhattacharya A, Ventra M D, et al. Electrostatic modification of novel materials. Rev Mod Phys, 2006, 78: 1185–1212
14 Wang J L, Mckinstry S T. Oxygen vacancy motion in Er-doped barium strontium titanate thin films. Appl Phys Lett, 2006, 89: 172906
15 Chen G F, Li Z, Wu D, et al. Superconductivity at 41 K and its competition with spin-density-wave instability in layered $CeO_{1-x}F_xFeAs$. Phys Rev Lett, 2008, 100: 247002
16 Calvani P, Capizzi M, Donato F, et al. Observation of a midinfrared band in $SrTiO_{3-y}$. Phys Rev B, 1993, 47: 8917–8922
17 Kan D, Terashima T, Kanda R, et al. Blue-light emission at room temperature from Ar^+-irradiated $SrTiO_3$. Nat Mater, 2005, 4: 816–819
18 Sundaresan A, Bhargavi R, Rangarajan N, et al. Ferromagnetism as a universal feature of nanoparticles of the otherwise nonmagnetic oxides. Phys Rev B, 2006, 74: R161306
19 Shein I R, Ivanovskii A L. First principle prediction of vacancy-induced magnetism in non-magnetic perovskite $SrTiO_3$. Phys Lett A, 2007, 371: 155–159
20 Cuong D D, Lee B, Choi K M, et al. Oxygen vacancy clustering and electron localization in oxygen-deficient $SrTiO_3$: LDA+U study. Phys Rev Lett, 2007, 98: 115503
21 Li B Y, Zhou D X, Zhang D L, et al. Analysis on the aging characteristics of PTCR of donor-doped barium titanate. Mater Sci Eng B, 2003, 99: 394–398
22 Wang X X, Chan H L-W, Choy C-L. Positive temperature coefficient of resistivity effect in niobium-doped barium titanate ceramics obtained at low sintering temperature. J Eur Ceram Soc, 2004, 24: 1227–1231
23 Lu H B, Wang N, Chen W Z, et al. Laser molecular beam epitaxy of $BaTiO_3$ and $SrTiO_3$ ultra thin films. J Crystal Growth, 2000, 212: 173–177
24 Yang G Z, Lu H B, Wang H S, et al. Unit-cell by unit-cell epitaxial growth of $SrTiO_3$ and $BaTiO_3$ thin films by Laser Molecular Beam Epitaxy. Chin Phys Lett, 1997, 14: 478–480
25 Huang Y H, He M, Zhao K, et al. Laser molecular beam epitaxy growth of $BaTiO_3$ in seven thousands of unit-cell layers. Chin Phys Lett, 2005, 22: 2950–2952
26 Guo H Z, Liu L F, Lu H B, et al. Structure and transport properties of heteroepitaxial $BaNb_xTi_{1-x}O_3$ (x=0.05, 0.2) thin films. Thin Solid Films, 2006, 497: 341–346
27 Xing J, Jin K J, Lu H B, et al. Photovoltaic effects and its oxygen content dependence in $BaTiO_{3-\delta}$/Si heterojunctions. Appl Phys Lett, 2008, 92: 071113
28 Liu G Z, Jin K J, Qiu J, et al. Resistance switching in $BaTiO_{3-\delta}$/Si p-n heterostructure. Appl Phys Lett, 2007, 91: 252110